Eur. Phys. J. B **23**, 329–339 (2001)

THE EUROPEAN PHYSICAL JOURNAL B

EDP Sciences

Magnetic properties and spin waves of bilayer magnets in a uniform field

T. Sommer[1], M. Vojta[2,a], and K.W. Becker[1]

[1] Institut für Theoretische Physik, Technische Universität Dresden, 01062 Dresden, Germany
[2] Theoretische Physik III, Elektronische Korrelationen und Magnetismus, Institut für Physik, Universität Augsburg, 86135 Augsburg, Germany

Received 23 April 2001

Abstract. The two-layer square lattice quantum antiferromagnet with spins $\frac{1}{2}$ shows a zero-field magnetic order-disorder transition at a critical ratio of the inter-plane to intra-plane couplings. Adding a uniform magnetic field tunes the system to canted antiferromagnetism and eventually to a fully polarized state; similar behavior occurs for ferromagnetic intra-plane coupling. Based on a bond operator spin representation, we propose an approximate ground state wavefunction which consistently covers all phases by means of a unitary transformation. The excitations can be efficiently described as independent bosons; in the antiferromagnetic phase these reduce to the well-known spin waves, whereas they describe gapped spin-1 excitations in the singlet phase. We compute the spectra of these excitations as well as the magnetizations throughout the whole phase diagram.

PACS. 73.43.Nq Quantum phase transitions – 75.10.Jm Quantized spin models – 75.50.Ee Antiferromagnetics

1 Introduction

Bilayer quantum magnets have attracted much interest in experiment and theory in recent years, especially in the context of quantum Hall systems and of quasi-two dimensional transition metal oxides. On the experimental side, quantum Hall systems [1] are especially suitable for investigating zero temperature quantum transitions between states with different spin magnetizations. In particular, bilayer quantum Hall systems at filling fraction $\nu = 2$ [2–4] can be tuned between a fully polarized, ferromagnetic state and a spin singlet ground state as function of the layer distance. It is now well established [2,5–7] that there is not a first-order ferromagnet-singlet transition, but rather an intermediate phase with *canted* spin ordering bounded by second-order transitions. The spin degrees of freedom therefore appear to be well described by a bilayer quantum spin model [8]. On the other hand, transition metal oxides like cuprates are known to form two-dimensional structures where the low-energy spin dynamics is well described by a Heisenberg model. These materials consist either of a single plane or a stack of copper oxide planes with intervening charge reservoir layers. Prominent examples for bilayer compounds are $YBa_2Cu_3O_{7-x}$ and $Bi_2Sr_2CaCu_2O_{8+\delta}$ which show a number of unusual properties [9]. Note that in the high-temperature superconductors the interlayer coupling is relatively weak compared to intralayer processes; undoped bilayer systems like $YBa_2Cu_3O_6$ are not driven into a singlet ground state. However, the latter is also possible: recently the material $BaCuSi_2O_6$ containing strongly coupled bilayers has been discovered and investigated [10], it shows a spin gap due to strong antiferromagnetic exchange interaction between the two layers.

On the theoretical side, the bilayer Heisenberg magnet has attracted a lot of interest [8,11–25] because it is a simple model for studying the interplay of long-range magnetic order and quantum disorder. Quantum-critical behavior associated with such a magnetic instability has been observed, *e.g.*, in the cuprate superconductors over a wide range of doping levels and temperatures [26].

We start by describing the bilayer quantum Heisenberg model. The system consists of two planes of nearest-neighbor $S = \frac{1}{2}$ Heisenberg models with coupling constant $J_\parallel$ which can be either antiferromagnetic ($J_\parallel > 0$) or ferromagnetic ($J_\parallel < 0$). The spins of corresponding sites of each layer are coupled antiferromagnetically with a coupling constant $J_\perp > 0$. The Hamiltonian reads

$$\mathcal{H} = J_\perp \sum_i \mathbf{S}_{i1}\cdot\mathbf{S}_{i2} + J_\parallel \sum_{\langle ij\rangle m} \mathbf{S}_{im}\cdot\mathbf{S}_{jm} - \mathbf{B}\cdot\sum_{im}\mathbf{S}_{im} \quad (1)$$

where $\mathbf{S}_{im}$ are the electronic spin operators. The index i denotes *rungs* of the bilayer lattice, and $m = 1, 2$ labels the planes. The summation $\langle ij\rangle$ runs over pairs of nearest-neighbor rungs. The external magnetic field $\mathbf{B}$ is homogeneous, the Zeeman interaction factors $g_J\mu_B$ (gyromagnetic

[a] e-mail: matthias.vojta@physik.uni-augsburg.de

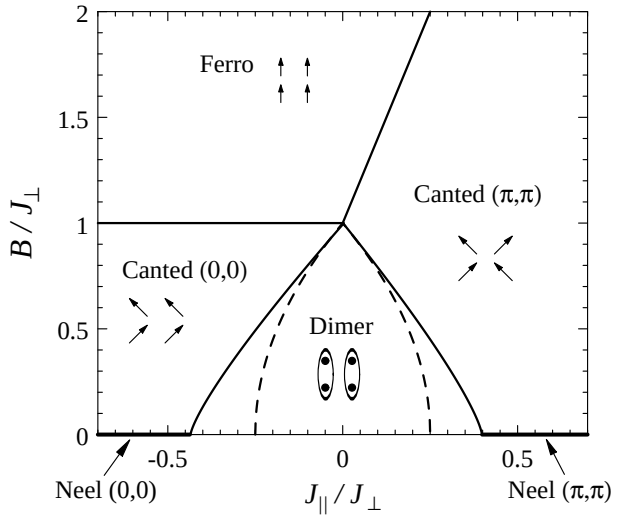

Fig. 1. Ground state phase diagram of $\mathcal{H}$ (1) as determined from series expansion studies, see references [8,15,20]. The arrows denote the spin orientations, the in-plane ordering wavevectors are given in brackets. The dashed lines are the boundaries of the singlet phase obtained from the lowest-order boson approximation as described in Section 3.

ratio and Bohr magneton) have been absorbed in the definition of $\mathbf{B}$.

In the following, we briefly discuss the main features of the ground-state phase diagram of the model (1), which has been given in two recent papers [8,15] and is shown in Figure 1. In the absence of a magnetic field the bilayer Heisenberg antiferromagnet is known to exhibit quantum phase transitions between a disordered singlet phase and long-range ordered (LRO) phases. In the limit of strong interplanar coupling, $J_\perp \gg |J_\parallel|$, the system consists of weakly interacting rung singlets, and the ground state possesses the full symmetry of the Hamiltonian. The spin excitations are triplet modes with a minimum energy gap Δ, there is no magnetic LRO. In the opposite case of large $|J_\parallel|/J_\perp$, the system possesses LRO at $T = 0$, the ordering wavevector is $(0, 0, \pi)$ $[(\pi, \pi, \pi)]$ for ferromagnetic (antiferromagnetic) $J_\parallel$. The SU(2) symmetry of $\mathcal{H}$ is broken, the low-lying excitations are doubly-degenerate Goldstone spin waves. The quantum transitions between the singlet and the two ordered phases are of the O(3) universality class [11,12,18,23] and occur at critical ratios $(J_\perp/J_\parallel)_{c1,2}$. For the antiferromagnetic case, quantum Monte Carlo calculations [11,12,25], series expansions [13], and the diagrammatic Brueckner approach [14] yield an order-disorder transition point of $(J_\parallel/J_\perp)_{c1} = 0.396$. Bond-operator mean-field theory applied to the bilayer Heisenberg AF [15,16] gives a transition point of $(J_\parallel/J_\perp)_{c1} = 0.435$. Note that Schwinger boson mean-field theory [17] predicts a value of $(J_\parallel/J_\perp)_{c1} \approx 0.22$, and also self-consistent spin-wave theory [18,19], which yields $(J_\parallel/J_\perp)_{c1} \approx 0.23$, fails to reproduce the numerical results. As Chubukov and Morr [18] have pointed out this discrepancy is due to the neglect of longitudinal spin fluctuations in the conventional spin-wave approach. For ferromagnetic $J_\parallel < 0$, the series expansion result is $(J_\parallel/J_\perp)_{c2} = -0.435$ which agrees well with the value from bond-operator mean-field theory.

For large enough external field, $\mathbf{B} = B\mathbf{e_z}$, the exact ground state is the fully polarized ferromagnetic (FPF) state, *i.e.*, the state with all spins pointing in the direction of the applied field. The first excited state is a single spin flip and its excitation energy can be determined exactly: $\omega_{\mathbf{k}} = B - J_\perp - J_\parallel(2 - \cos k_x - \cos k_y)$. For ferromagnetic (antiferromagnetic) intra-plane coupling $J_\parallel$ the minimum of $\omega_{\mathbf{k}}$ is located at in-plane wavevector $\mathbf{Q} = (0, 0)$ $[\mathbf{Q} = (\pi, \pi)]$. The stability boundary of the FPF state is given by the point where the minimum excitation energy vanishes, this yields the exact expression for the upper critical field, $B_{c2} = J_\perp$ $[B_{c2} = 4J_\parallel + J_\perp]$ for ferromagnetic (antiferromagnetic) $J_\parallel$. Single spin flips condense at this boundary, leading to canted spin ordering. The transition is of second order and in the universality class of the dilute Bose gas quantum-critical point with $z = 2$ [6–8,15,27]. For intermediate magnetic fields a canted spin phase is established which breaks the rotational symmetry of the Hamiltonian about the z axis, leading to one linear dispersing Goldstone mode corresponding to a rotation of the order parameter in the x-y plane. Both the expectation value of the uniform magnetization in field direction and the $\mathbf{Q}$-staggered magnetization perpendicular to the field are non-zero.

For small uniform fields, $B < \Delta$, the disordered spin singlet ground state discussed above remains unchanged due to its finite excitation gap Δ. The effect of the magnetic field is simply to split the degenerate triplet excitations due to Zeeman coupling, $\omega_{\mathbf{k}} \to \omega_{\mathbf{k}} - mB$, where $m = -1, 0, 1$ is the S_z quantum number. The stability boundary of the singlet phase is determined by the vanishing of the excitation gap; the corresponding transition is in the same universality class as the boundary of the fully polarized phase, also leading to the same canted phase with ordering vector $\mathbf{Q}$.

The purpose of the present paper is to propose a transformation of the usual bond operator basis which allows an efficient description of *all* phases described above. In the simplest approximation, the excitations can be described as independent bosons. In the limit of weak inter-plane coupling, the approach then reduces to linear spin-wave theory, with the surplus of correctly describing the gapped *longitudinal* amplitude mode which corresponds to inter-plane quantum fluctuations and becomes important near the transition to a singlet state. The paper is organized as follows: In Section 2 we introduce the bond operator transformation which is employed to describe the magnetic phases of the bilayer model. Section 3 is devoted to the boson approximation which can be used to diagonalize the Hamiltonian *via* a Bogoliubov transformation. Results for ground state magnetizations and excitation spectra are given in Section 4. A summary and discussion of possible improvements beyond the independent boson approximation close the paper.

2 Generalized bond operators

The four spin states per rung can be conveniently described *via* a bond operator representation [28] of the two spins $\mathbf{S}_{i1}$ and $\mathbf{S}_{i2}$ of each rung i. We introduce bosonic bond operators for creation of a singlet and three triplet states out of the vacuum $|0\rangle$:

$$\begin{aligned}
s_i^\dagger|0\rangle &= \frac{1}{\sqrt{2}}(c_{i1,\uparrow}^\dagger c_{i2,\downarrow}^\dagger - c_{i1,\downarrow}^\dagger c_{i2,\uparrow}^\dagger)|0\rangle = \frac{1}{\sqrt{2}}(|\uparrow\downarrow\rangle - |\downarrow\uparrow\rangle)\\
t_{ix}^\dagger|0\rangle &= \frac{-1}{\sqrt{2}}(c_{i1,\uparrow}^\dagger c_{i2,\uparrow}^\dagger - c_{i1,\downarrow}^\dagger c_{i2,\downarrow}^\dagger)|0\rangle = \frac{-1}{\sqrt{2}}(|\uparrow\uparrow\rangle - |\downarrow\downarrow\rangle)\\
t_{iy}^\dagger|0\rangle &= \frac{i}{\sqrt{2}}(c_{i1,\uparrow}^\dagger c_{i2,\uparrow}^\dagger + c_{i1,\downarrow}^\dagger c_{i2,\downarrow}^\dagger)|0\rangle = \frac{\mathrm{i}}{\sqrt{2}}(|\uparrow\uparrow\rangle + |\downarrow\downarrow\rangle)\\
t_{iz}^\dagger|0\rangle &= \frac{1}{\sqrt{2}}(c_{i1,\uparrow}^\dagger c_{i2,\downarrow}^\dagger + c_{i1,\downarrow}^\dagger c_{i2,\uparrow}^\dagger)|0\rangle = \frac{1}{\sqrt{2}}(|\uparrow\downarrow\rangle + |\downarrow\uparrow\rangle)
\end{aligned} \tag{2}$$

where $c_{im\sigma}^\dagger$ are creation operators for electrons at site im with spin σ. In terms of the bond operators the spin operators can be expressed as

$$S_{i1,2}^\alpha = \frac{1}{2}(\pm s_i^\dagger t_{i\alpha} \pm t_{i\alpha}^\dagger s_{\mathrm{i}} - i\epsilon_{\alpha\beta\gamma} t_{i\beta}^\dagger t_{i\gamma}). \tag{3}$$

A local constraint of the form

$$s_i^\dagger s_i + \sum_\alpha t_{i\alpha}^\dagger t_{i\alpha} = 1 \tag{4}$$

has to be imposed on each rung to ensure that the physical states are either singlets or triplets. The ground state for vanishing intra-plane coupling, $J_\parallel = 0$, is given by the product state of singlet bonds on each rung, *i.e.*,

$$|\phi_0\rangle = \prod_i s_i^\dagger|0\rangle\ . \tag{5}$$

In this limit, the excitations are localized triplets with an energy gap $J_\perp$.

Substituting the bond operator representation of the spin operators (3) into the original Heisenberg model we obtain the following Hamiltonian [29–31]:

$$\begin{aligned}
\mathcal{H}_0 &= -\frac{3}{4}J_\perp \sum_i s_i^\dagger s_i + \frac{1}{4}J_\perp \sum_{i\alpha} t_{i\alpha}^\dagger t_{i\alpha}\,,\\
\mathcal{H}_1 &= \frac{J_\parallel}{2}\sum_{\langle ij\rangle,\alpha}(t_{i\alpha}^\dagger s_j^\dagger t_{j\alpha} s_i + \mathrm{h.c.})\\
&\quad + \frac{J_\parallel}{2}\sum_{\langle ij\rangle,\alpha}(t_{i\alpha}^\dagger t_{j\alpha}^\dagger s_i s_j + \mathrm{h.c.})\\
&\quad + \frac{J_\parallel}{2}\sum_{\langle ij\rangle,\alpha,\beta}(t_{i\alpha}^\dagger t_{j\beta}^\dagger t_{j\alpha} t_{i\beta} - t_{i\alpha}^\dagger t_{j\alpha}^\dagger t_{i\beta} t_{j\beta})\\
&\quad + \mathrm{i}B\sum_i (t_{ix}^\dagger t_{iy} - t_{iy}^\dagger t_{ix}).
\end{aligned} \tag{6}$$

In the following the basic idea of describing the various magnetic phases will be discussed. Starting from the singlet phase, the magnetically ordered phases can be described by different triplet boson condensates [18,31,32]. The FPF phase with polarization in z direction requires a condensate of $(t_x + \mathrm{i}t_y)$ bosons; a Néel state with staggered magnetization perpendicular to the field corresponds to a condensate of t_x or t_y on top of the singlet state. Neglecting inter-rung fluctuations, an ansatz wavefunction can be written as

$$\begin{aligned}
|\tilde{\phi}_0\rangle &\sim \exp(\mathrm{i}\mu\sum_i t_{iy}^\dagger t_{ix})\exp(\lambda\sum_i \mathrm{e}^{\mathrm{i}\mathbf{Q}\mathbf{R}_i} t_{ix}^\dagger s_i)|\phi_0\rangle\\
&= \prod_i (s_i^\dagger + \lambda \mathrm{e}^{\mathrm{i}\mathbf{Q}\mathbf{R}_i}(t_{ix}^\dagger + \mathrm{i}\mu t_{iy}^\dagger))|0\rangle.
\end{aligned} \tag{7}$$

The real parameters λ and μ are the condensation amplitudes, $\mathbf{Q}$ denotes the in-plane ordering wavevector. This ansatz contains two subsequent unitary transformations of the singlet product state $|\phi_0\rangle$ (5): the λ term creates a spin-density-wave condensate with ordering vector $\mathbf{Q}$ and quantization axis in x direction (thus explicitely breaking the U(1) symmetry of the z axis rotation), the μ term introduces canting and a non-zero z magnetization into this state. For $\mu = 0$ and $\mathbf{Q} = (\pi, \pi)$ which corresponds to $J_\parallel > 0$ and $B = 0$, this wavefunction reduces to a state interpolating between the singlet and the Néel state; it has been recently used to describe the dynamics of holes doped into a bilayer system [31]. A finite external field B larger than the spin gap will lead to a finite uniform magnetization described by finite μ; for large B the system is driven into a fully polarized state with $\lambda \to \infty$ and $\mu = 1$. The intervening canted phase will be characterized by finite, non-zero λ and $0 < \mu < 1$.

A related product state has recently been employed for the description of bilayer quantum Hall systems [7], with the inclusion of charge fluctuations and additional disorder, but without inter-rung spin fluctuations. We will show here that such spatial correlations can be efficiently described in a simple harmonic theory.

For a proper description of fluctuations around the product state $|\tilde{\phi}_0\rangle$ (7) it is convenient to transform the basis states on each rung. We replace the basis operators $\{s_i, t_{i\alpha}\}$ by

$$\begin{aligned}
\tilde{s}_i^\dagger &= \frac{1}{\sqrt{1+\lambda^2}}\left(s_i^\dagger + \frac{\lambda \mathrm{e}^{\mathrm{i}\mathbf{Q}\mathbf{R}_\mathbf{i}}}{\sqrt{1+\mu^2}}(t_{ix}^\dagger + \mathrm{i}\mu t_{iy}^\dagger)\right),\\
\tilde{t}_{ix}^\dagger &= \frac{1}{\sqrt{1+\lambda^2}}\left(-\lambda \mathrm{e}^{\mathrm{i}\mathbf{Q}\mathbf{R}_\mathbf{i}} s_i^\dagger + \frac{1}{\sqrt{1+\mu^2}}(t_{ix}^\dagger + \mathrm{i}\mu t_{iy}^\dagger)\right),\\
\tilde{t}_{iy}^\dagger &= \frac{1}{\sqrt{1+\mu^2}}\left(t_{iy}^\dagger + \mathrm{i}\mu t_{ix}^\dagger\right),\\
\tilde{t}_{iz}^\dagger &= t_{iz}^\dagger.
\end{aligned} \tag{8}$$

The constraint (4) takes the form $\tilde{s}_i^\dagger \tilde{s}_i + \sum_\alpha \tilde{t}_{i\alpha}^\dagger \tilde{t}_{i\alpha} = 1$. The new product state $|\tilde{\phi}_0\rangle$ can now be written as

$$|\tilde{\phi}_0\rangle = \prod_i \tilde{s}_i^\dagger|0\rangle \tag{9}$$

which reduces to the singlet product state for $\lambda = 0$. Excitations out of this state are given by $\tilde{t}^\dagger_{i\alpha}\tilde{s}_i$. At this point it is worth emphasizing that the use of a *single* condensate (of "mixed" $\tilde{s}$ bosons) and the basis transformation to excitation operators being *orthogonal* to $\tilde{s}$ is crucial for a correct description of the ordered phases.

We can now insert the new basis operators into (6) and obtain the expression for the transformed Hamiltonian $\tilde{\mathcal{H}}$:

$$
\begin{aligned}
\tilde{\mathcal{H}}_0 &= \sum_{i\alpha} H(\alpha;\alpha)\ \tilde{t}^\dagger_{i\alpha}\tilde{t}_{i\alpha} + \sum_i H(s;s)\ \tilde{s}^\dagger_i\tilde{s}_i \\
&\quad + \sum_i H(x;y)\ \mathrm{i}(\tilde{t}^\dagger_{ix}\tilde{t}_{iy} - \tilde{t}^\dagger_{iy}\tilde{t}_{ix})\,, \\
\tilde{\mathcal{H}}_1 &= \sum_i H(x;s)\ (\tilde{t}^\dagger_{ix}\tilde{s}_i + \tilde{s}^\dagger_i\tilde{t}_{ix}) \\
&\quad + \sum_i H(y;s)\ \mathrm{i}(\tilde{t}^\dagger_{iy}\tilde{s}_i - \tilde{s}^\dagger_i\tilde{t}_{iy}) \\
&\quad + \sum_{\langle ij\rangle} H(ss;ss)\ \tilde{s}^\dagger_i\tilde{s}^\dagger_j\tilde{s}_i\tilde{s}_j \\
&\quad + \sum_{\langle ij\rangle\alpha} H(\alpha\alpha;ss)\ \tilde{t}^\dagger_{i\alpha}\tilde{t}^\dagger_{j\alpha}\tilde{s}_i\tilde{s}_j + \text{h.c.} \\
&\quad + \sum_{\langle ij\rangle} H(xy;ss)\ \tilde{t}^\dagger_{ix}\tilde{t}^\dagger_{jy}\tilde{s}_i\tilde{s}_j + \text{h.c.} + i \leftrightarrow j \\
&\quad + \sum_{\langle ij\rangle\alpha} H(\alpha s;s\alpha)\ \tilde{t}^\dagger_{i\alpha}\tilde{t}_{j\alpha}\tilde{s}^\dagger_j\tilde{s}_i + \text{h.c.} \\
&\quad + \sum_{\langle ij\rangle} H(xs;sy)\ \tilde{t}^\dagger_{ix}\tilde{t}_{jy}\tilde{s}^\dagger_j\tilde{s}_i + \text{h.c.} + i \leftrightarrow j \\
&\quad + \sum_{\langle ij\rangle} H(xs;xs)\ \tilde{t}^\dagger_{ix}\tilde{t}_{ix}\tilde{s}^\dagger_j\tilde{s}_j + i \leftrightarrow j \\
&\quad + \sum_{\langle ij\rangle} H(ys;ys)\ \tilde{t}^\dagger_{iy}\tilde{t}_{iy}\tilde{s}^\dagger_j\tilde{s}_j + i \leftrightarrow j \\
&\quad + \sum_{\langle ij\rangle} H(xs;ys)\ \tilde{t}^\dagger_{ix}\tilde{t}_{iy}\tilde{s}^\dagger_j\tilde{s}_j + i \leftrightarrow j \\
&\quad + \sum_{\langle ij\rangle} H(xs;ss)\ \left(\tilde{t}^\dagger_{ix}\tilde{s}_i\tilde{s}^\dagger_j\tilde{s}_j + \tilde{s}^\dagger_j\tilde{t}_{ix}\tilde{s}^\dagger_j\tilde{s}_j\right) + i \leftrightarrow j \\
&\quad + \sum_{\langle ij\rangle} H(ys;ss)\ \left(\tilde{t}^\dagger_{iy}\tilde{s}_i\tilde{s}^\dagger_j\tilde{s}_j + \tilde{s}^\dagger_j\tilde{t}_{iy}\tilde{s}^\dagger_j\tilde{s}_j\right) + i \leftrightarrow j \\
&\quad + \tilde{\mathcal{H}}_{\text{rest}}. \qquad (10)
\end{aligned}
$$

The coefficients $H(\cdot,\cdot)$ depend on the basis parameters λ and μ as well as on $J_\parallel$, $J_\perp$, and B; explicit expression are given in Appendix A. $\tilde{\mathcal{H}}_{\text{rest}}$ contains more complicated terms with three and four excitations. In the case of $\mu = 0$ the Hamiltonian reduces to the Hamiltonian derived for the zero-field case [31]. It can be seen that $\tilde{\mathcal{H}}_1$ contains creation, hopping, and conversion terms of the three types of excitations $\{\tilde{t}_{ix}, \tilde{t}_{iy}, \tilde{t}_{iz}\}$. Contrary to the original Hamiltonian $\mathcal{H}_1$ where the triplet excitations can only occur in pairs, here also single $\tilde{t}_{ix}$ and $\tilde{t}_{iy}$ excitations can be created. The effect of these terms is directly related to the basis parameters λ and μ and will be used to determine their values. In contrast to the case of zero field where only pairs of the same type of excitation are created out of $|\tilde{\phi}_0\rangle$, for any finite B also pairs of the structure $\tilde{t}^\dagger_{ix}\tilde{t}^\dagger_{jy}\tilde{s}_i\tilde{s}_j$ are present.

The exact but lengthy representation (10) can now be used for a variety of approximation schemes. The most important point is to choose values for λ and μ in such a way that the product state $|\tilde{\phi}_0\rangle$ (9) is a reasonable starting point for approximations. Fluctuations are described by the hard-core bosons $\{\tilde{t}_{ix}, \tilde{t}_{iy}, \tilde{t}_{iz}\}$, and a "good" choice for $|\tilde{\phi}_0\rangle$ should ensure that the ground-state density of the bosons is small. The lowest-order approximation corresponds to independent bosons with a bilinear Hamiltonian, it is formally given by ignoring both the hard-core constraint (4) as well as $\tilde{\mathcal{H}}_{\text{rest}}$, and assuming a complete condensation of the generalized "singlet", *i.e.*, $\langle\tilde{s}\rangle = \tilde{s} = 1$. This approximation will be discussed in the following sections, it is shown to correspond to usual linear spin-wave theory in the decoupled plane limit with $B = 0$. Possible improvements include (i) taking into account the site-averaged constraint by introduction of a chemical potential λ_0, and treating λ_0 and $\tilde{s}$ as variational parameters in the spirit of bond-operator mean-field theory [15,16], (ii) a mean-field-like factorization of the higher-order boson interaction terms (iii) a diagrammatic treatment of the hard-core boson interaction in the framework of Brueckner theory [14]. Independently, methods focusing on higher-order local excitations based on cumulants [31] or the coupled-cluster technique [33] known from quantum chemistry may be applied to (10).

3 Independent boson approximation

In this and the following section, we will discuss the lowest-order boson approximation for the Hamiltonian (10). For this purpose we treat the excitations $\{\tilde{t}_{ix}, \tilde{t}_{iy}, \tilde{t}_{iz}\}$ as independent bosons, *i.e.*, neglect the constraint which restricts the Hilbert space per rung. The (generalized) singlet is assumed to fully condense, $\langle\tilde{s}\rangle = 1$. It is known from the zero-field case [14,31] that this approximation is controlled by the existence of a small parameter, namely the density of (generalized) triplet excitations $\langle\tilde{t}^\dagger_{i\alpha}\tilde{t}_{i\alpha}\rangle$. With this in mind, all terms of the Hamiltonian containing more than two excitation operators $\tilde{t}_{i\alpha}$ will be neglected.

The parameters of the unitary transformation λ and μ have not yet been determined. Within the approximation of independent bosons these parameters are chosen so that the prefactors of the terms creating single $\tilde{t}_{i\alpha}$ bosons out of $|\tilde{\phi}_0\rangle$ vanish. The physical meaning of this is easily understood: terms creating single bosons would change the condensate densities (and therefore alter the effective values of λ and μ), however, our aim is to fully account for the boson condensation by the transformed basis state $|\tilde{\phi}_0\rangle$. One arrives at the following non-linear equations for

the basis parameters λ and μ:

$$\lambda^2 = \frac{\left[\pm 4J_\parallel - J_\perp(1+\mu^2) + 2B\mu\right](1+\mu^2)}{\left[\pm 4J_\parallel + J_\perp(1+\mu^2) - 2B\mu\right](1+\mu^2) + 8J_\parallel\mu^2}$$
$$0 = B(1-\mu^4)(1+\lambda^2) \mp 4J_\parallel\mu(1+\mu^2) - 4J_\parallel\lambda^2\mu(1-\mu^2) \tag{11}$$

where upper (lower) sign refers to $J_\parallel > 0$ ($J_\parallel < 0$). Notably, these equations also follow from a variational principle, *i.e.*, they are obtained by minimizing $\langle\tilde{\phi}_0|\mathcal{H}|\tilde{\phi}_0\rangle$ with respect to λ and μ. This clarifies the meaning of $|\tilde{\phi}_0\rangle$ as best variational state without inter-rung fluctuations.

The system of nonlinear equations (11) allows for the computation of the phase boundaries. The rotational invariant spin singlet phase is characterized by the value $\lambda = 0$. Solutions for μ are then obtained for $B < B_{\rm c1}$, where $B_{\rm c1}$ is the stability boundary of the singlet phase:

$$B_{\rm c1} = \sqrt{J_\perp - 4J_\parallel} \quad (J_\parallel > 0)\,,$$
$$B_{\rm c1} = \sqrt{J_\perp + 4J_\parallel} \quad (J_\parallel < 0)\,. \tag{12}$$

It can be seen that the singlet phase exists for $|J_\parallel/J_\perp| < 0.25$. At the critical ratio $(J_\parallel/J_\perp)_{\rm c} = \pm 0.25$ the character of the zero-field ground state changes from spin singlet to long-range order. As discussed in reference [23], this *quasi-classical* value of $(J_\parallel/J_\perp)_{\rm c}$ is necessarily smaller than the exact one (quantum fluctuations stabilize the inter-plane singlet phase); as noted in the introduction the critical values obtained by large-scale numerics are $(J_\parallel/J_\perp)_{\rm c1} = 0.396$ and $(J_\parallel/J_\perp)_{\rm c2} = -0.435$. The inclusion of higher order terms beyond the present linear "spin-wave" approximation leads to a better agreement with the numerical values for the critical coupling ratio [31].

For values of the field with $B_{\rm c1} < B < B_{\rm c2}$ the ground state is a canted phase with $0 < \mu < 1$. The phase boundary to the ferromagnetic phase is obtained when the limit $\lambda \to \infty$ and $\mu \to 1$ is taken. We arrive at an upper critical field of

$$B_{\rm c2} = J_\perp + 4J_\parallel \quad (J_\parallel > 0)\,,$$
$$B_{\rm c2} = J_\perp \quad (J_\parallel < 0) \tag{13}$$

which are the exact results.

We can now proceed with analyzing the fluctuations around $|\tilde{\phi}_0\rangle$. With the approximations described above, we arrive at a bilinear Hamiltonian:

$$\begin{aligned}\tilde{\mathcal{H}} = &\sum_{\mathbf{k}\alpha} A_{\mathbf{k}\alpha}\tilde{t}^\dagger_{\mathbf{k}\alpha}\tilde{t}_{\mathbf{k}\alpha} \\ &+ \frac{1}{2}\sum_{\mathbf{k}\alpha} B_{\mathbf{k}\alpha}\left(\tilde{t}^\dagger_{\mathbf{k}\alpha}\tilde{t}^\dagger_{-\mathbf{k}\alpha} + \tilde{t}_{\mathbf{k}\alpha}\tilde{t}_{-\mathbf{k}\alpha}\right) \\ &+ \sum_{\mathbf{k}} C_{\mathbf{k}}\left(\tilde{t}^\dagger_{\mathbf{k}x}\tilde{t}_{\mathbf{k}y} - \tilde{t}^\dagger_{\mathbf{k}y}\tilde{t}_{\mathbf{k}x}\right) \\ &+ \sum_{\mathbf{k}} D_{\mathbf{k}}\left(\tilde{t}^\dagger_{\mathbf{k}x}\tilde{t}^\dagger_{-\mathbf{k}y} - \tilde{t}_{\mathbf{k}x}\tilde{t}_{-\mathbf{k}y}\right)\,. \end{aligned} \tag{14}$$

Here, $\tilde{t}_{\mathbf{k}\alpha}$ are the modified basis operators which have been Fourier transformed with respect to the in-plane momentum $\mathbf{k}$. The expressions for the coefficients $A_{\mathbf{k}}, \ldots, D_{\mathbf{k}}$ can be found in Appendix B. The Hamiltonian (14) can be easily diagonalized with a Bogoliubov transformation, leading to new generalized excitations denoted by $\tau_{\mathbf{k}\alpha}$, $\alpha = x, y, z$. The ground state $|\psi_0\rangle$ is simply the vacuum of the bosons $\tau_{\mathbf{k}\alpha}$. The excitation energies of these bosons are given by

$$\begin{aligned}\Omega^2_{\mathbf{k}x,y} = &\frac{1}{2}\left(\omega^2_{\mathbf{k}x} + \omega^2_{\mathbf{k}y} - 2C^2_{\mathbf{k}} + 2D^2_{\mathbf{k}}\right) \\ &\pm \Big\{ \frac{1}{4}\left(\omega^2_{\mathbf{k}x} + \omega^2_{\mathbf{k}y} - 2C^2_{\mathbf{k}} + 2D^2_{\mathbf{k}}\right)^2 \\ &- \omega^2_{\mathbf{k}x}\omega^2_{\mathbf{k}y} - \left(C^2_{\mathbf{k}} - D^2_{\mathbf{k}}\right)^2 \\ &+ 2\left(\left(A_{\mathbf{k}x}A_{\mathbf{k}y} - B_{\mathbf{k}x}B_{\mathbf{k}y}\right)\left(C^2_{\mathbf{k}} + D^2_{\mathbf{k}}\right)\right. \\ &\left. -2\left(A_{\mathbf{k}x}B_{\mathbf{k}y} - A_{\mathbf{k}y}B_{\mathbf{k}x}\right)C_{\mathbf{k}}D_{\mathbf{k}}\right) \Big\}^{\frac{1}{2}}, \\ \Omega^2_{\mathbf{k}z} = &A^2_{\mathbf{k}z} - B^2_{\mathbf{k}z}\,, \end{aligned} \tag{15}$$

the terms $\omega^2_{\mathbf{k}x} := A^2_{\mathbf{k}x} - B^2_{\mathbf{k}x}$ and $\omega^2_{\mathbf{k}y} := A^2_{\mathbf{k}y} - B^2_{\mathbf{k}y}$ are simply the eigenenergies of the zero field limit. In zero field, we find either three degenerate gapped modes in the singlet phase, or two degenerate transverse acoustic spin-wave modes and a gapped spin-amplitude mode in the long-range ordered phases. A finite external field lifts these degeneracies; the canted phase supports a single Goldstone mode due to the broken U(1) symmetry. Explicit results for the dispersion relations are shown in the next section.

Finally the ground state energy per site is given by the expression

$$E_g = \frac{\langle\psi_0|\tilde{\mathcal{H}}|\psi_0\rangle}{2N} = E_0 + \frac{1}{2N}\sum_{\mathbf{k}\alpha}(\Omega_{\mathbf{k}\alpha} - A_{\mathbf{k}\alpha}) \tag{16}$$

where E_0 is the energy per site of the product state $|\tilde{\phi}_0\rangle$, $E_0 = \langle\tilde{\phi}_0|\mathcal{H}|\tilde{\phi}_0\rangle/2N$.

The described harmonic approximation preserves SU(2) symmetry in the singlet phase; in the ordered phases it can be considered as linear spin-wave theory for the bilayer problem with inclusion of *longitudinal* spin fluctuations [18,32,34] – these are crucial for describing the magnetic properties near the boundary to the singlet phase. For zero field and vanishing inter-plane coupling, $B = J_\perp = 0$, the results of the present approach are equivalent to the ones of linear spin-wave theory. For instance, in the antiferromagnetic case, the magnetization takes 60 % of its classical value. There, the gapped amplitude mode is dispersionless and does not influence the ground state properties, and its spectral weight in neutron scattering vanishes.

4 Ground state properties and spin excitations

In this section we present the results obtained from the independent boson approximation. We discuss the staggered

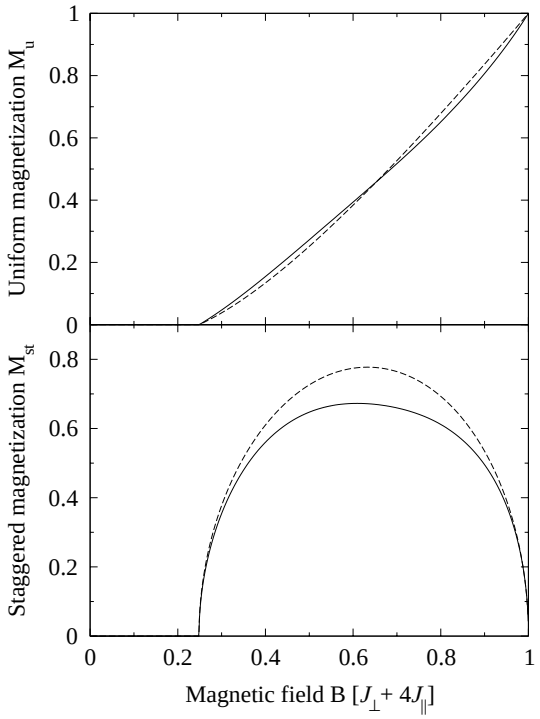

Fig. 2. Uniform (top) and staggered magnetization (bottom) as function of the external magnetic field B/B_{c2}. The ratio of the coupling constants $J_\parallel/J_\perp = 0.2$ which places the zero-field system into the interlayer singlet phase. Solid: present approximation (independent bosons). Dashed: product wavefunction $|\tilde{\phi}_0\rangle$ only.

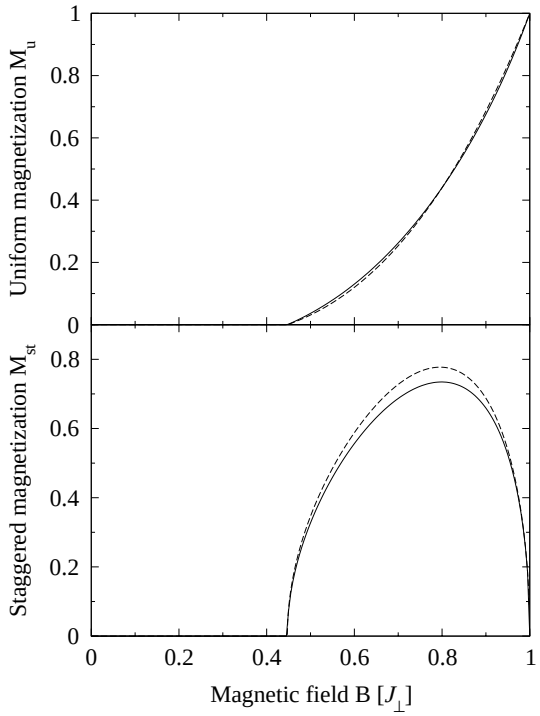

Fig. 3. As Figure 2, but in the singlet phase with strongly coupled *ferromagnetic* planes with $J_\parallel/J_\perp = -0.2$.

and uniform magnetizations and the dispersion relations as functions of the external magnetic field in order to characterize the various magnetic phases. For this purpose we consider the system for small intra-plane coupling $|J_\parallel|$, *i.e.*, in the singlet phase, as well as for weakly coupled planes (small $J_\perp$).

4.1 Magnetization

We start with the uniform and staggered magnetizations which are obtained as expection values of the corresponding spin operators

$$M_{\rm u} = \frac{1}{N}\sum_i \langle S^z_{i1} + S^z_{i2}\rangle\,,$$
$$M_{\rm st} = \frac{1}{N}\sum_i \langle S^x_{i1} - S^x_{i2}\rangle e^{i\mathbf{Q}\mathbf{R}_i} \qquad (17)$$

where $\mathbf{Q} = (0,0)$ [$\mathbf{Q} = (\pi,\pi)$] for ferromagnetic (antiferromagnetic) intra-plane coupling $J_\parallel$ as above. The staggered magnetization in the zero-field case has been calculated earlier (see Fig. 2 of Ref. [31]); it shows a good overall agreement with the series expansion data of reference [13] if plotted as function of $(J_\parallel/J_\perp)/(J_\parallel/J_\perp)_{\rm c}$ – the critical coupling ratio itself is underestimated in the independent boson approach as discussed above.

Turning to the finite-B case, we show uniform and staggered magnetization in Figures 2–5. Both are zero in the singlet phase, $B < B_{c1}$. Varying the magnetic field from the lower critical value B_{c1} to the upper critical field B_{c2} the uniform magnetization increases from 0 and saturates at B_{c2}, whereas the staggered magnetization is nonzero only in the canted phase, $B_{c1} < B < B_{c2}$, passing a maximum in between (Figs. 2, 3). Near the critical fields

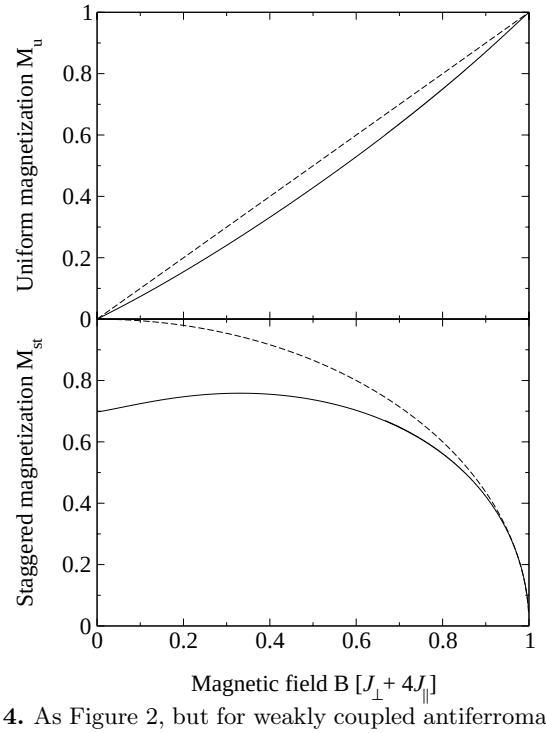

Fig. 4. As Figure 2, but for weakly coupled antiferromagnetic planes with $J_\parallel/J_\perp = 10$.

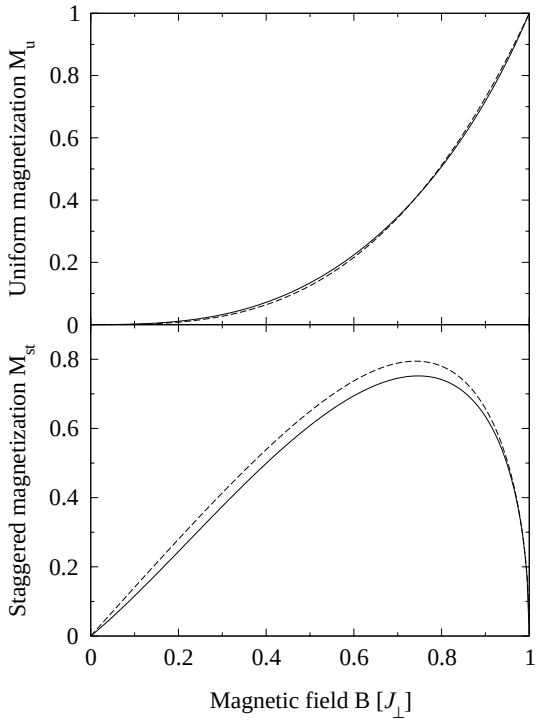

Fig. 5. As Figure 2, now at the zero-field critical point between the singlet and "ferromagnetic" $\mathbf{Q} = (0, 0)$ Néel phase, $J_\parallel/J_\perp = -0.25$ (see Fig. 1).

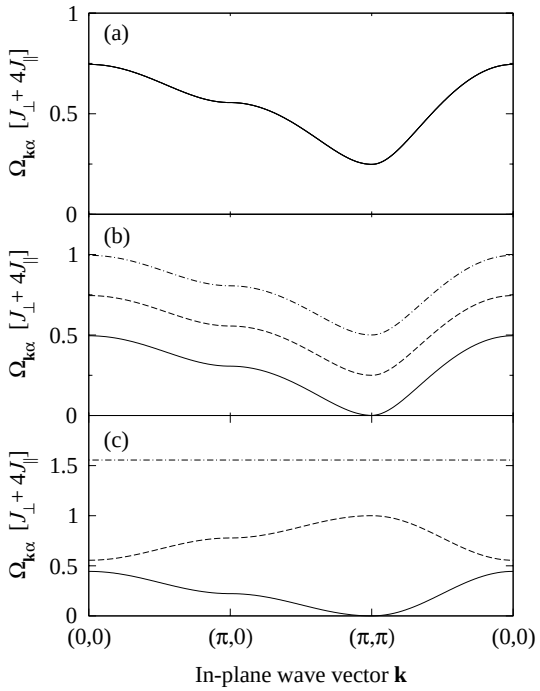

Fig. 6. Dispersion relations of the magnetic excitations for strongly coupled antiferromagnetic planes, $J_\parallel/J_\perp = 0.2$. The three panels show the three modes for different magnetic fields $\tilde{B} = B/B_{c2} = B/(4J_\parallel + J_\perp)$, (a) $\tilde{B} = 0$, (b) $\tilde{B} = 0.44$ (here $B = B_{c1}$), (c) $\tilde{B} = 1$ ($B = B_{c2}$).

for $B \gtrsim B_{c1}$ or $B \lesssim B_{c2}$, we have $M_u \sim |B - B_{c1,2}|$ and $M_{st} \sim |B - B_{c1,2}|^{1/2}$.

For small $J_\perp$, *i.e.*, in the zero-field ordered regime, the staggered magnetization M_{st} is finite at $B = 0$ but is suppressed if B is increased up to the critical field B_{c2}, see Figure 4. Interestingly, M_{st} increases (!) at small fields – here the suppression of quantum fluctuations due to the field (*e.g.* one Goldstone mode becomes gapped) has a stronger effect than the change in the canting angle. The uniform magnetization again increases continuously with B until it saturates at B_{c2}. For illustration, we also show data for $J_\parallel/J_\perp = -0.25$ which places the model at the zero-field critical point between the singlet and $\mathbf{Q} = (0, 0)$ Néel phases. Here, M_u increases with B^2 whereas M_{st} raises linearly with the applied field, in agreement with the results of reference [6].

In Figures 2–5, we have also shown the magnetization values calculated with the product state $|\tilde{\phi}_0\rangle$ only (dashed lines) – this is equivalent to neglecting intra-plane (inter-rung) fluctuations altogether. It can be seen that the effect of these spatial quantum fluctuations is largest for antiferromagnetic $J_\parallel$ and large staggered magnetization, this includes the case of the single-layer antiferromagnet where quantum fluctuations are known to reduce M_{st} by 40%. In contrast, in both the ferromagnetic regime (where quantum fluctuations are weak in general) and near the spin singlet phase (where *inter-plane* quantum fluctuations dominate), the effect of intra-plane fluctuations is weaker.

All phase transitions found are of second order, as expected, except for the special point $J_\parallel = 0$, $B = J_\perp$, where the singlet–FPF transition is a simple level crossing for independent rungs. Due to the mean-field character of the present approximation, all critical exponents have mean-field values. (It is easily seen that the present harmonic approximation becomes exact in the limit of large in-plane coordination number, see also Ref. [23].) For the actual two-dimensional model, these mean-field exponents are incorrect for the zero-field transitions which have $z = 1$ and therefore obey the non-trivial exponents of a three-dimensional classical Heisenberg model, but they apply (ignoring logarithmic corrections) to the field-induced transitions from and to the canted phase which are at the upper-critical dimension ($z = 2$) [6–8,27].

We note that the phase boundaries obtained in Section 3 using the product state $|\tilde{\phi}_0\rangle$ are *not* changed by the inclusion of inter-rung fluctuations at the lowest boson level employed here. It is, however, clear that boson interactions change this picture [14].

4.2 Magnetic excitations

We continue with the discussion of the dispersion relations of the magnetic excitations, plotted in Figures 6–9, for a number of values of the external field. In Figure 6 we show data for strongly coupled planes and antiferromagnetic $J_\parallel$. In the zero-field limit (Fig. 6a) the excitations are threefold degenerate, gapped, and have a dispersion minimum at $\mathbf{Q} = (\pi, \pi)$. At finite B, the degeneracy is lifted due to the Zeeman coupling. At the lower critical

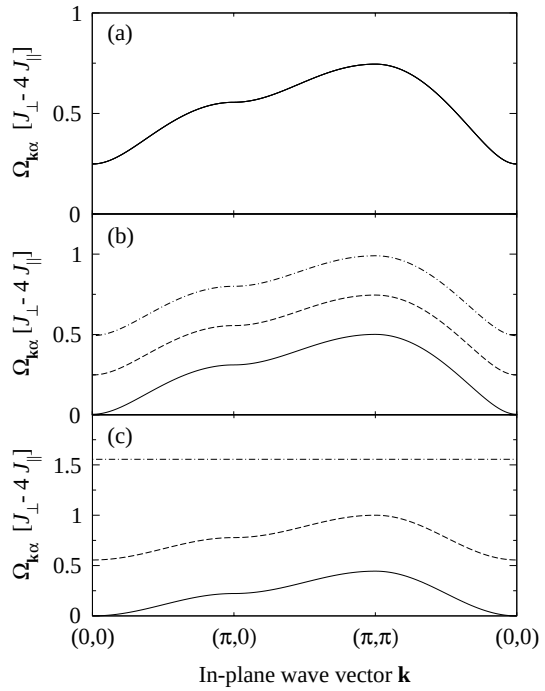

Fig. 7. As in Figure 6, but for ferromagnetic in-plane coupling, $J_\parallel/J_\perp = -0.2$. Note that the magnetic field values in units of B_{c2} are again $\tilde{B} = 0$, 0.44, and 1, but here $B_{c2} = J_\perp$, *i.e.*, $\tilde{B} = B/J_\perp$.

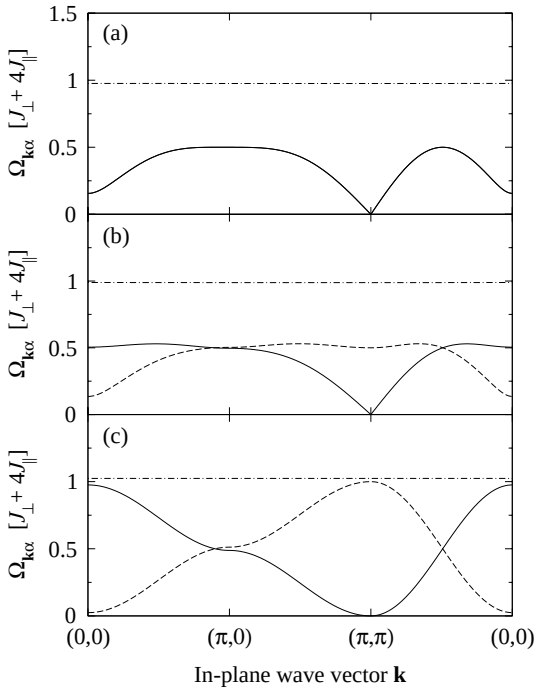

Fig. 8. As in Figure 6, here for weakly coupled antiferromagnetic planes, $J_\parallel/J_\perp = 10$.

field, $B = B_{c1}$ (Fig. 6b), the excitation gap closes, and there is a single critical mode with quadratic dispersion. In the canted phase, $B_{c1} < B < B_{c2}$ (not shown), there is a single Goldstone mode with a linear dispersion around $\mathbf{Q} = (\pi, \pi)$, corresponding to the broken $U(1)$ symmetry. At the phase boundary to the ferromagnetic (FPF) phase, $B = B_{c2}$ (Fig. 6c), the lowest mode becomes again critical with a quadratic dispersion (note $z = 2$ at both field-induced transitions). As the magnetic field is further increased, a gap opens and the FPF phase is stabilized. In the FPF phase, one of the excitations is dispersionless, corresponding to a longitudinal local fluctuation which turns both spins on a rung down. In the case of ferromagnetic in-plane coupling, $J_\parallel < 0$, the picture is similar, but the dispersion minimum is now found at $\mathbf{Q} = (0, 0)$, see Figure 7.

The results for weakly coupled antiferromagnetic planes are plotted in Figure 8. We start with a discussion of the zero field case, shown in Figure 8a. Contrary to the case of strong inter-plane coupling there is now a nearly dispersionless excitation – this is the beforementioned gapped (longitudinal) spin-amplitude mode. It corresponds to flipping both spins on a single rung and has a quantum number $S^z = 0$, consequently, it remains unchanged (to linear order) when the magnetic field is turned on. The two other modes are degenerate Goldstone bosons in the zero-field limit with a linear dispersion around the ordering wavevector $\mathbf{Q} = (\pi, \pi)$. For decoupled planes, $J_\perp \to 0$, momenta $(0, 0)$ and (π, π) are degenerate, and for small $J_\perp$ the gap at $(0, 0)$ is proportional to $J_\perp$. With increasing $J_\perp$, the spin-amplitude mode acquires a dispersion, until it merges with the acoustic spin-wave modes at the zero-field critical point, leading to a degenerate triplet of critical modes with linear dispersion (not shown). Turning to the case of a finite uniform field B, we note that arbitrarily small B establishes canted ordering here. For $0 < B < B_{c2}$ (Fig. 8b), the mode degeneracy is again lifted and leaves a single gapless Goldstone excitation with linear dispersion. At $B = B_{c2}$ (Fig. 8c), this mode becomes critical with quadratic dispersion as discussed above.

Finally, Figure 9 shows dispersions for the coupling ratio corresponding to the zero-field ferromagnetic critical point, $J_\parallel/J_\perp = -0.25$. For $B = 0$ (Fig. 9a), we have a triplet of degenerate critical modes with minimum (condensation) wavevector $\mathbf{Q} = (0, 0)$ and a linear dispersion reflecting $z = 1$. With application of a finite field, we enter directly the canted phase with a single Goldstone mode, so for Figures 9b, c the above discussion applies.

At this point a remark about the physics of longitudinal magnon mode is in order. As mentioned, this mode is not included in conventional spin-wave theory for the antiferromagnet. The reason is that spin-wave theory has the character of a $1/S$ expansion, and longitudinal fluctuations are suppressed in the $S \to \infty$ limit. This implies that any theory based on a (finite-order) large-S expansion can never treat longitudinal and transverse spin fluctuations on equal footing [18], which is, however, crucial near the critical point in the bilayer model where longitudinal and transverse fluctuations become indistinguishable. In contrast, our approach preserves the quantum nature of the

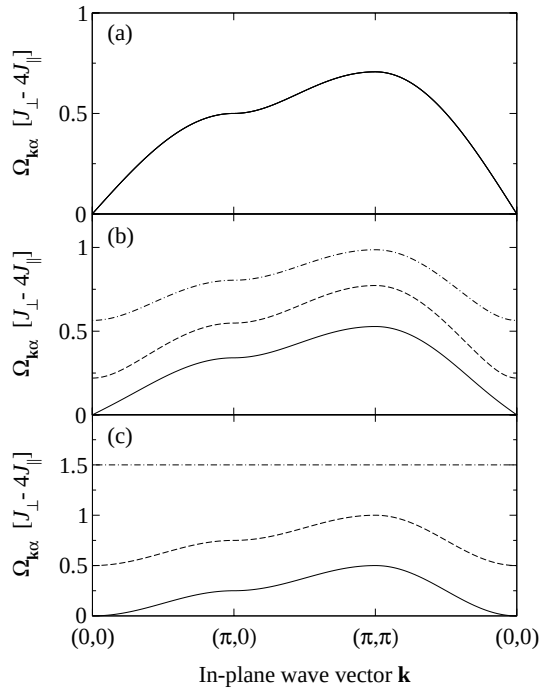

Fig. 9. As in Figure 7, finally for the coupling constant ratio $J_\parallel/J_\perp = -0.25$, corresponding to the zero-field critical point on the ferromagnetic side of the phase diagram (Fig. 1).

$S = 1/2$ spins, but has the spirit of a large-z theory, where z is the in-plane coordination number.

We close this section with some general remarks. The lowest-order boson approximation neglects interactions between the modes, therefore all excitations including the amplitude mode are undamped, and no decay into the two-particle continuum is possible. The description of such damping processes requires the inclusion of fourth-order boson terms, and is deferred to future investigation.

The low-energy properties of the spin excitations obtained in the present work are in agreement with hydrodynamical considerations. The spin-wave velocity c in an ordered phase, defined as $\Omega_{\mathbf{q}} = c\,|\mathbf{q} - \mathbf{Q}|$ near the ordering wavevector $\mathbf{Q}$, has to fulfill the relation $c^2 = \rho_\mathrm{s}/\chi_\perp$ where ρ_s is the spin stiffness and $\chi_\perp$ denotes the uniform susceptibility for a field perpendicular to the ordering direction (here x). At the zero-field transitions, $J_\parallel/J_\perp = (J_\parallel/J_\perp)_{\mathrm{c}1,2}$, both ρ_s and $\chi_\perp$ vanish whereas c remains non-critical as expected for an O(3) transition. This behavior is correctly reproduced in our calculations (Figs. 5 and 9), note $\chi_\perp = \mathrm{d}M_\mathrm{u}/\mathrm{d}B$. (In contrast, at the field-induced transition points the spin-wave velocity c vanishes, leading to a quadratically dispersing critical mode at $B = B_{\mathrm{c}1,2}$.)

The special properties of the multicritical points at $B = 0$, $J_\parallel/J_\perp = (J_\parallel/J_\perp)_{\mathrm{c}1,2}$ have been discussed in reference [8]. One consequence of universal scaling arguments is that the energy gap of the $B = 0$ amplitude mode in the ordered phase close to the transition is given by the spin stiffness ρ_s; this result is special to $d = 2$ where ρ_s has the dimension of energy. We also note that a well-defined amplitude mode requires that the low-energy theory for the zero-field ordering transition is below its upper-critical dimension (here $d_{\mathrm{c,up}} = 3$) so that the interaction term of the effective ϕ^4 theory is relevant in the renormalization group sense. Our mean-field theory gives an amplitude mode independent of the spatial dimension d, but from the above it is clear that even the low-energy part of this mode will be overdamped from boson interactions in higher dimensions, $d \geq 3$.

The results obtained with the present method for vanishing inter-plane coupling, $J_\perp = 0$, are consistent with recent calculations using linear spin-wave theory [35] for a single-plane antiferromagnet.

5 Conclusion

In this paper, we have proposed a unitary transformation of bond-boson operators appropriate for the description of various magnetic phases, especially with canted spin order. The resulting boson Hamiltonian has been obtained exactly; it allows for a number of approximations. We have applied this method to the bilayer Heisenberg magnet in a uniform external field. Using the lowest-order approximation of free bosons we obtained analytic expressions for the phase boundaries, the quasiparticle excitations and both uniform and staggered magnetization. The harmonic approximation is controlled by the smallness of the density of generalized bosonic triplet excitations, this parameter has been found to be smaller than 0.15 throughout the whole phase diagram. In the limit of vanishing inter-plane coupling, the boson approximation reduces to linear spin-wave theory; near the transition to the singlet phase it has the advantage of incorporating *longitudinal* spin fluctuations. The phase diagram (Fig. 1) is adequately described; the locations of the zero-field transitions are $(J_\parallel/J_\perp)_{\mathrm{c}1,2} = \pm 0.25$, these values are smaller in magnitude than the ones obtained by more accurate numerical and analytical methods ($(J_\parallel/J_\perp)_{\mathrm{c}1} = 0.396$ and $(J_\parallel/J_\perp)_{\mathrm{c}2} = -0.435$). These deviations arise from the neglect of boson interactions which stabilize the singlet phase. The approach presented here preserves all general properties expected from hydrodynamics, *i.e.*, it gives the correct number and low-energy dispersion of Goldstone modes in the symmetry-broken phases.

The present approximation can be systematically improved as discussed in Section 2. Two promising possibilities are either the inclusion of fourth-order boson terms as in non-linear spin-wave theory or the treatment of the hard-core boson constraint by introduction of an (infinite) on-site repulsion which is treated diagrammatically using Brueckner theory [14]. (The latter approach yields very accurate results for the zero-field bilayer antiferromagnet.) We expect that the inclusion of interactions will induce a damping of the high-energy spin excitation modes, but will not change the low-energy properties presented in Section 4 which are protected by symmetry considerations and hydrodynamics. Once interactions are included, a detailed study of the dynamic structure factor as measured in inelastic neutron scattering, including the

spectral weights of the excitation modes described here, would be interesting.

We close by mentioning possible applications of the present approach. As in reference [31], it can be used for studying a hole- or electron doped system; in this case the ground state wavefunction derived here can be used as a background state for the carrier motion. Other interesting prospectives include the study of disorder [7] and the application to *frustrated* systems in the presence of an external field. A nice example here is the recently discovered triangular bilayer $S = 1$ system $Ba_3Mn_2O_8$ which shows a spin gap, magnetization plateaus, and interesting frustration effects [36].

The authors acknowledge useful discussions with C. Kühnert, K. Meyer, and S. Sachdev as well as financial support by the DFG (SFB 463 and 484).

Appendix A: Hamiltonian in the modified bond boson basis

In the following, we list the first terms appearing in the transformed bilayer Hamiltonian $\tilde{\mathcal{H}}$ (10) for antiferromagnetic $J_\parallel$.

$$H(s;s) = \left(J_\perp + 2B\frac{\mu}{1+\mu^2}\right)\frac{\lambda^2}{1+\lambda^2},$$

$$H(x;x) = \left(J_\perp + 2B\frac{\mu}{1+\mu^2}\right)\frac{1}{1+\lambda^2},$$

$$H(y;y) = J_\perp + 2B\frac{\mu}{1+\mu^2}\ , \quad H(z;z) = J_\perp,$$

$$H(x;s) = \left(J_\perp - 2B\frac{\mu}{1+\mu^2}\right)\frac{\lambda \mathrm{e}^{\mathrm{i}\mathbf{Q}\mathbf{R}_i}}{1+\lambda^2},$$

$$H(y;s) = B\frac{1-\mu^2}{1+\mu^2}\frac{\lambda \mathrm{e}^{\mathrm{i}\mathbf{Q}\mathbf{R}_i}}{\sqrt{1+\lambda^2}},$$

$$H(x;y) = \frac{-B}{\sqrt{1+\lambda^2}}\frac{1-\mu^2}{1+\mu^2},$$

$$H(xx;ss) = \frac{J_\parallel}{2}\frac{(1+\mu^2)\left[\left(1-\lambda^2\right)^2 + \mu^2\left(1+\lambda^2\right)^2\right] - 4\lambda^2\mu^2}{\left(1+\lambda^2\right)^2\left(1+\mu^2\right)^2},$$

$$H(yy;ss) = \frac{J_\parallel}{2}\ \frac{\left(1-\mu^2\right)\left[\left(1+\mu^2\right) + \lambda^2\left(1-\mu^2\right)\right]}{\left(1+\lambda^2\right)\left(1+\mu^2\right)^2},$$

$$H(zz;ss) = \frac{J_\parallel}{2}\ \frac{\left(1+\mu^2\right) + \lambda^2\left(1-\mu^2\right)}{\left(1+\lambda^2\right)\left(1+\mu^2\right)}\ .$$

These and the remaining terms can be obtained with the help of *Mathematica* by inserting the transformation (8) into $\mathcal{H}$ (6).

Appendix B: Bilinear Hamiltonian

We list here the coefficients of the bilinear boson Hamiltonian (14) which enter the expressions for the dispersions given in (15). For shortness, we restrict ourselves to the antiferromagnetic case, $J_\parallel > 0$, and use the abbreviation $\gamma_{\mathbf{k}} = \frac{1}{2}\left(\cos k_x + \cos k_y\right)$.

$$\begin{aligned} A_{\mathbf{k}x} = &\left(J_\perp - \frac{2B\mu}{1+\mu^2}\right)\frac{1-\lambda^2}{1+\lambda^2} \\ &+8J_\parallel\frac{\lambda^2\left(2+3\mu^2-\lambda^2\mu^2\right)}{\left(1+\lambda^2\right)^2\left(1+\mu^2\right)^2} \\ &+2J_\parallel\gamma_{\mathbf{k}}\frac{\left(1-\lambda^2\right)^2\left(1+2\mu^2\right)+\left(1+\lambda^2\right)^2\mu^4}{\left(1+\lambda^2\right)^2\left(1+\mu^2\right)^2}, \end{aligned}$$

$$\begin{aligned} A_{\mathbf{k}y} = &J_\perp\frac{1}{1+\lambda^2} + 2B\mu\frac{1+2\lambda^2}{\left(1+\lambda^2\right)\left(1+\mu^2\right)} \\ &+8J_\parallel\frac{\lambda^2\left(1-2\lambda^2\mu^2\right)}{\left(1+\lambda^2\right)^2\left(1+\mu^2\right)^2} \\ &+2J_\parallel\gamma_{\mathbf{k}}\frac{\left(1+\mu^2\right)^2-\lambda^2\left(1-\mu^2\right)^2}{\left(1+\lambda^2\right)\left(1+\mu^2\right)^2}, \end{aligned}$$

$$\begin{aligned} A_{\mathbf{k}z} = &J_\perp\frac{1}{1+\lambda^2} + 2B\mu\frac{\lambda^2}{\left(1+\lambda^2\right)\left(1+\mu^2\right)} \\ &+8J_\parallel\frac{\lambda^2\left(1+\mu^2\left(1-\lambda^2\right)\right)}{\left(1+\lambda^2\right)^2\left(1+\mu^2\right)^2} + 2J_\parallel\gamma_{\mathbf{k}}\left(\frac{1-\lambda^2}{1+\lambda^2}\right), \end{aligned}$$

$$B_{\mathbf{k}x} = 2J_\parallel\gamma_{\mathbf{k}}\frac{\left(1-\lambda^2\right)^2-\left(1+\lambda^2\right)^2\mu^4-8\lambda^2\mu^2}{\left(1+\lambda^2\right)^2\left(1+\mu^2\right)^2},$$

$$B_{\mathbf{k}y} = 2J_\parallel\gamma_{\mathbf{k}}\frac{\left(1-\mu^4\right)+\lambda^2\left(1-\mu^2\right)^2}{\left(1+\lambda^2\right)\left(1+\mu^2\right)^2},$$

$$B_{\mathbf{k}z} = 2J_\parallel\gamma_{\mathbf{k}}\frac{\left(1+\lambda^2\right)+\left(1-\lambda^2\right)\mu^4+2\mu^2}{\left(1+\lambda^2\right)\left(1+\mu^2\right)^2},$$

$$\begin{aligned} \frac{C_{\mathbf{k}}}{\mathrm{i}} = &B\frac{1-\mu^2}{1+\mu^2}\frac{1}{\sqrt{1+\lambda^2}} \\ &+8J_\parallel\frac{\lambda^2\mu^3}{\left(1+\lambda^2\right)^{3/2}\left(1+\mu^2\right)^2}\left(1-\gamma_{\mathbf{k}}\right), \end{aligned}$$

$$\frac{D_{\mathbf{k}}}{\mathrm{i}} = -4J_\parallel\gamma_{\mathbf{k}}\frac{\mu}{\left(1+\lambda^2\right)^{3/2}\left(1+\mu^2\right)}\left(1+\lambda^2\frac{1-\mu^2}{1+\mu^2}\right).$$

In the zero field case ($B = 0$, $\mu = 0$) we have $C_{\mathbf{k}} = D_{\mathbf{k}} = 0$, and therefore $\Omega_{\mathbf{k}x} = \omega_{\mathbf{k}x}$, $\Omega_{\mathbf{k}y} = \omega_{\mathbf{k}y}$. In the FPF phase ($B > B_{c2}$, $\lambda = \infty$, $\mu = 1$) we find $B_{\mathbf{k}} = C_{\mathbf{k}} = D_{\mathbf{k}} = 0$, and the Hamiltonian (14) is already diagonal in the $\tilde{t}_{\mathbf{k}\alpha}$ operators.

References

1. *Perspectives in Quantum Hall Effects*, edited by S. Das Sarma, A. Pinczuk (Wiley, New York, 1997).
2. V. Pellegrini *et al.*, Phys. Rev. Lett. **78**, 310 (1997), Science **281**, 799 (1998).
3. A. Sawada, Z.F. Ezawa, H. Ohno, Y. Horikoshi, Y. Ohno, S. Kishimoto, F. Matsukura, M. Yasumoto, A. Urayama, Phys. Rev. Lett. **80**, 4534 (1998).

4. K. Yang, Phys. Rev. B **60**, 15578 (1999); A.H. MacDonald, R. Rajaraman, T. Jungwirth, Phys. Rev. B **60**, 8817 (1999).
5. A. Pinczuk *et al.* Bull. Am. Phys. Soc. **41**, 482 (1996); A.S. Plaut, *ibid.* **41**, 590 (1996).
6. L. Zheng, R.J. Radtke, S. Das Sarma, Phys. Rev. Lett. **78**, 2453 (1997); S. Das Sarma, S. Sachdev, L. Zheng, Phys. Rev. B **58**, 4672 (1998).
7. E. Demler, S. Das Sarma, Phys. Rev. Lett. **82**, 3895 (1999).
8. M. Troyer, S. Sachdev, Phys. Rev. Lett. **81**, 5418 (1998).
9. A.J. Millis, H. Monien, Phys. Rev. Lett. **70**, 2810 (1993).
10. Y. Sasago, K. Uchinokura, A. Zheludev, G. Shirane, Phys. Rev. B **55**, 8357 (1997).
11. A.W. Sandvik, D.J. Scalapino, Phys. Rev. Lett. **72**, 2777 (1994).
12. A.W. Sandvik, A.V. Chubukov, S. Sachdev, Phys. Rev. B **51**, 16483 (1995).
13. W.H. Zheng, Phys. Rev. B **55**, 12267 (1997).
14. V.N. Kotov, O.P. Sushkov, W.H. Zheng, J. Oitmaa, Phys. Rev. Lett. **80**, 5790 (1998).
15. Y. Matsushita, M.P. Gelfand, C. Ishii, J. Phys. Soc. Jpn **68**, 247 (1999).
16. D.-K. Yu, Q. Gu, H.-T. Wang, J.-L. Shen, Phys. Rev. B **59**, 111 (1999).
17. A.J. Millis, H. Monien, Phys. Rev. B **50**, 16606 (1994).
18. A.V. Chubukov, D. Morr, Phys. Rev. B **52**, 3521 (1995).
19. K. Hida, J. Phys. Soc. Jpn **59**, 2230 (1990), *ibid.* **61**, 1013 (1992).
20. M.P. Gelfand, Phys. Rev. B **53**, 11309 (1996).
21. K.K. Ng, F.C. Zhang, M. Ma, Phys. Rev. B **53**, 12196 (1996).
22. N. Elstner, R.R.P. Singh, Phys. Rev. B **57**, 7740 (1998).
23. C.N.A. van Duin, J. Zaanen, Phys. Rev. Lett. **78**, 3019 (1997).
24. Q. Gu, D.-K. Yu, J.-L. Shen, Phys. Rev. B **60**, 3009 (1999).
25. P.V. Shevchenko, A.W. Sandvik, O.P. Sushkov, Phys. Rev. B **61**, 3475 (2000).
26. Y. Uemura, Phys. Rev. Lett. **66**, 2665 (1991); T. Imai *et al.*, Phys. Rev. Lett. **70**, 1002 (1993); M. Takigawa, Phys. Rev. B **49**, 4158 (1994); G. Aeppli, T.E. Mason, S.M. Hayden, H.A. Mook, J. Kulda, Science **278**, 1432 (1997).
27. S. Sachdev, T. Senthil, Ann. Phys. (New York) **251**, 76 (1996).
28. S. Sachdev, R.N. Bhatt, Phys. Rev. B **41**, 9323 (1990).
29. S. Gopalan, T.M. Rice, M. Sigrist, Phys. Rev. B **49**, 8901 (1994).
30. R. Eder, Phys. Rev. B **57**, 12832 (1998).
31. M. Vojta, K.W. Becker, Phys. Rev. B **60**, 15201 (1999).
32. B. Normand, T.M. Rice, Phys. Rev. B **56**, 8760 (1997); see also: B. Normand, Acta Phys. Pol. B **31**, 3005 (2000).
33. For recent applications of the coupled-cluster technique to spin systems see: R.F. Bishop, D.J.J. Farnell, J.B. Parkinson, Phys. Rev. B **58**, 6394 (1998); R.F. Bishop *et al.*, Int. J. Mod. Phys. B **15**, 1385 (2001), `cond-mat/0011008` (2000).
34. For an early discussion of longitudinal modes in one-dimensional antiferromagnets see: I. Affleck, Phys. Rev. Lett. **62**, 474 (1989); I. Affleck, G.F. Wellman, Phys. Rev. B **46**, 8934 (1992).
35. M.E. Zhitomirsky, T. Nikuni, Phys. Rev. B **57**, 5013 (1998).
36. M. Uchida, H. Tanaka, M. Bartashevich, T. Goto, J. Phys. Soc. Jpn **70**, 1790 (2001), `cond-mat/0102026` (2001).